

Complexes of Atmospheric α -Dicarbonyls with Water: FTIR Matrix Isolation and Theoretical Study

Malgorzata Mucha and Zofia Mielke*

Faculty of Chemistry, University of Wrocław, Joliot-Curie 14, 50-383 Wrocław, Poland

Received: October 11, 2006; In Final Form: January 17, 2007

The complexes of glyoxal (Gly), methylglyoxal (MGly), and diacetyl (Dac) with water have been studied using Fourier transform infrared (FTIR) matrix isolation spectroscopy and MP2 calculations with 6-311++G-(2d,2p) basis set. The analysis of the experimental spectra of the Gly(MGly,Dac)/H₂O/Ar matrixes indicates formation of one Gly···H₂O complex, three MGly···H₂O complexes, and two Dac···H₂O ones. All the complexes are stabilized by the O–H···O(C) hydrogen bond between the water molecule and carbonyl oxygen as evidenced by the strong perturbation of the O–H, C=O stretching vibrations. The blue shift of the CH stretching vibration in the Gly···H₂O complex and in two MGly···H₂O ones suggests that these complexes are additionally stabilized by the improper C–H···O(H₂) hydrogen bonding. The theoretical calculations confirm the experimental findings. They evidence the stability of three hydrogen-bonded Gly···H₂O and Dac···H₂O complexes and six MGly···H₂O ones stabilized by the O–H···O(C) hydrogen bond. The calculated vibrational frequencies and geometrical parameters indicate that one Dac···H₂O complexes, two Gly···H₂O, and three MGly···H₂O ones are additionally stabilized by the improper hydrogen bonding between the C–H group and water oxygen. The comparison of the theoretical frequencies with the experimental ones allowed us to attribute the calculated structures to the complexes present in the matrixes.

Introduction

Hydrocarbons containing carbonyl groups play an important role in atmospheric chemistry. The simple carbonyl-containing compounds formaldehyde, acetaldehyde, and acetone are important sources of HO_x in the troposphere.^{1–3} The photo-oxidation of aromatic hydrocarbons, that are emitted into the atmosphere in urban and industrial areas, leads to formation of the simple α -dicarbonyls glyoxal, methylglyoxal, and diacetyl.⁴ Various carbonyl compounds are found in relatively high concentrations in polluted water droplets.^{5,6}

The binary complex between water and formaldehyde may serve as a model for water carbonyl group interactions and has been a subject of very intense theoretical studies.^{7–24} Kumpf and Damewood⁸ reported the most complete data obtained by high-level ab initio calculations on various possible configurations of the water–formaldehyde complex in its ground state. The detailed infrared matrix isolation studies of the formaldehyde–water complex in inert matrixes^{25,26} indicated the formation of the complex with the O···H–O hydrogen bond between the CO and OH groups. The experimental data suggested that the complex exists in two isomeric forms with different relative orientations of the two interacting molecules. Fourier transform infrared (FTIR) matrix isolation studies of the binary complex between water and acetone indicated a structure in which water is hydrogen bonded to the carbonyl oxygen of acetone.²⁷ Ab initio SCF calculations performed for this complex²⁷ demonstrated a cyclic hydrogen-bonded structure involving, in addition to the O–H···O(C) bond, a weak C–H···O(H₂) interaction between one methyl hydrogen and water oxygen atom. The complex has been more recently studied by help of the DFT method; however, the work focused on the solvent shifts of the complex infrared spectrum.²⁸

Methylglyoxal, in addition to its role in atmospheric chemistry, plays also an important role in biological systems,²⁹ and its behavior in water has been recently the subject of detailed studies.³⁰ The behavior of glyoxal in water solution has been also the subject of numerous studies.^{31,32} However, to our knowledge, there are neither theoretical nor experimental data on the binary complexes between water and simple α -dicarbonyls glyoxal, methylglyoxal, and diacetyl. These complexes may play a role in the chemistry of atmosphere. In addition, the data concerning the water–methylglyoxal interaction may be important for understanding the biological activity of methylglyoxal. This work was undertaken to obtain information on the binary complexes between water and glyoxal, methylglyoxal, or diacetyl molecules. We performed FTIR studies of the complexes isolated in low-temperature matrixes and supported them with ab initio calculations at the MP2/6-311++G(2d,2p) level of theory.

Experimental Section

Infrared Matrix Isolation Studies. Monomeric glyoxal CHOCHO was prepared by heating the solid trimer dihydrate (98%, Sigma) topped with P₄O₁₀ powder under vacuum to 120 °C and by collecting the gaseous monomer in a trap at 77 K. From a 40% aqueous solution of methylglyoxal CH₃COCHO (Aldrich), the major amount of water was distilled off in a vacuum line. The residue was depolymerized at about 90 °C, and the product was passed through P₄O₁₀ and was trapped at 77 K. The sample was stored at liquid nitrogen temperature. Diacetyl CH₃COCOCH₃ (97%, Aldrich) was carefully outgassed and vacuum distilled, discarding the most volatile and the least volatile impurities. The dicarbonyl/Ar, H₂O/Ar, and dicarbonyl/H₂O/Ar mixtures were prepared by the standard manometric technique; the concentration of mixtures varied in the range 4/1/2400–1/1/150. The gas mixtures were sprayed onto gold-plated

* To whom correspondence should be addressed. E-mail: zm@wchuwr.chem.uni.wroc.pl.

TABLE 1: The Observed Frequencies and Calculated Frequency Shifts $\Delta\nu = \nu^{\text{complex}} - \nu^{\text{monomer}}$ (cm^{-1}) and Intensities^a (km/mol) for the $\text{H}_2\text{O}\cdots\text{CHOCHO}$ Complexes

experimental			calculated				assignment
M ^b	G _I		M ^b	gI	gII	gIII	
ν	ν	$\Delta\nu$	ν	$\Delta\nu$	$\Delta\nu$	$\Delta\nu$	
2861.2	2863.7	+2.5	3019(0)	+45	+36	+18	$\nu\text{C-H}$
2855.6	2858.1	+2.5	3014(101)	+13	+3	+19	
			1726(0)	-4	-3	-4	$\nu\text{C=O}$
1724.4	1717.8	-6.6	1713(125)	-9	-5	-5	
			1394(0)	+12	+5	+9	$\delta\text{C-H}$
1314.6	1322.6	+8	1357(6)	+10	+6	+8	
812.4							
806.7	808.1	+1.4	828(3)	+9	+11	+7	$\gamma\text{C-H}$
3735.0	3714.3	-20.7	3986(74)	-36	-31	-35	νOH
3638.0	3588.6	-49.4	3865(10)	-76	-67	-74	νOH
1590.0	1591.7	+1.7	1660(66)	+2	+3	+30	δHOH

^a The intensities are given in brackets. ^b The observed and calculated frequencies of the monomers are given for comparison.

copper mirror held at 17 K by a closed cycle helium refrigerator (Air Products, Displex 202A). Infrared spectra (resolution 0.5 cm^{-1}) were recorded in a reflection mode with Bruker 113v FTIR spectrometer using liquid N_2 cooled MCT detector.

Computational Details. The Gaussian 03 program³³ was used for geometry optimization and harmonic vibrational calculations. The structures of the isolated monomers (CHOCHO , $\text{CH}_3\text{-COCHO}$, $\text{CH}_3\text{COCOCH}_3$, and H_2O) and the structures of the dicarbonyl complexes with water were fully optimized by using the 6-311++G(2d,2p) basis set^{34,35} at the MP2 level.^{36,37} Vibrational frequencies and intensities were computed both for the monomers and for the complexes. Interaction energies were corrected by the Boys–Bernardi full counterpoise correction.³⁸

Results

Experimental Spectra. The infrared spectra of glyoxal in the gas phase³⁹ and in low-temperature matrixes have been reported;^{40,41} the molecule exists at standard conditions in the trans form. The spectra of diacetyl isolated in argon matrixes and in the solid state have been published recently,⁴² and it was shown that both in the crystalline phase and in the matrixes the compound exists in the trans conformation. The spectra of methylglyoxal in low-temperature matrixes have been the subject of recent studies in our laboratory and they are in accord with the reported gas phase spectra.⁴³ Like the other two simple α -dicarbonyls, the molecule exists at standard conditions in the trans conformation.⁴⁴ The spectra of water in low-temperature matrixes are well-known.^{45–48} Before the study of complexes was undertaken, the spectra of the parent molecules in argon matrixes were recorded, and they are in accord with the spectra previously reported.

When both water and α -dicarbonyl molecules are present in the matrixes, many new absorptions appeared in the vicinity of the glyoxal, methylglyoxal, diacetyl, and water monomer bands. The representative regions of the spectra of the Gly/ $\text{H}_2\text{O}/\text{Ar}$, MGly/ $\text{H}_2\text{O}/\text{Ar}$, and DAc/ $\text{H}_2\text{O}/\text{Ar}$ are shown in Figures 1–3. The frequencies of the observed product bands are presented in Tables 1–3.

Glyoxal–Water Complexes. In Figure 1, the region of the OH and C=O stretching vibrations in the spectra of Gly/ $\text{H}_2\text{O}/\text{Ar}$ is presented. Two new bands appear in the OH stretching region, at 3714.3 and 3588.6 cm^{-1} , and one new band in the C=O stretching region at 1717.8 cm^{-1} , when both glyoxal and water molecules are present in the matrix. The above absorptions are accompanied by the product bands in the C–H stretching, rocking, and wagging regions (at 2863.7, 2858.1, and 1322.6

and 808.1 cm^{-1} , respectively) and in the HOH bending region (at 1591.7 cm^{-1}). The new bands show small sensitivity to matrix annealing; their relative intensities were constant within an experimental error in all performed experiments.

Methylglyoxal–Water Complexes. The spectra of MGly/ $\text{H}_2\text{O}/\text{Ar}$ matrixes in the OH and C=O stretching regions are shown in Figure 2. Five new bands were observed in the water OH stretching region (at 3712.1, 3709.9, 3596.7, 3571.5, and 3561.7 cm^{-1}) and four in the C=O stretching one (at 1736.5, 1722.6, 1711.9, and 1705.3 cm^{-1}). As one can see in Figure 2, the new bands can be separated into two groups, M_I and M_{II}, on the basis of their response to matrix annealing. The bands attributed to group M_{II} increase and the bands assigned to group M_I disappear after matrix annealing. The 3709.9, 3561.7, and 3596.7 cm^{-1} bands and 1736.5 and 1711.9 cm^{-1} ones in the OH and C=O stretching regions, respectively, increase after matrix annealing and are attributed to the M_{II} group. The bands observed at 3712.1, 3571.5 cm^{-1} and at 1722.6, 1705.3 cm^{-1} strongly decrease when the matrix is warmed up and are assigned to the group M_I. In addition, careful spectra analysis allowed us to distinguish among the bands belonging to group M_{II} those which exhibit larger (M_{IIA}) and smaller (M_{IIIB}) intensity increase after annealing process; however, the separation into M_{IIA} and M_{IIIB} groups is not always evident, particularly for the weaker bands. The 3709.9, 3561.7, and 1711.9 cm^{-1} bands are assigned to M_{IIA} band set whereas the 3596.7 and 1736.5 cm^{-1} ones are assigned to the M_{IIIB} group. The bands belonging to the band sets M_I, M_{IIA}, and M_{IIIB} appear also in the other spectral regions; the frequencies of all observed bands are collected in Table 2.

Diacetyl–Water Complexes. Figure 3 shows the region of the water OH stretching and diacetyl C=O stretching vibrations in the spectra of DAc/ $\text{H}_2\text{O}/\text{Ar}$ matrixes. Three bands due to the perturbed water vibrations appear at 3708.3, 3582.8, and 3553.8 cm^{-1} and three bands due to the perturbed C=O stretches are observed at 1728.8, 1719.8, and 1715.8 cm^{-1} . After matrix annealing, the intensities of the 3553.8 cm^{-1} band and of the 1728.8 and 1715.8 cm^{-1} ones strongly increase whereas the 3582.8 cm^{-1} and 1719.8 cm^{-1} bands strongly diminish (they disappear after prolonged annealing). The intensity of the 3708.3 cm^{-1} band also increases but less than the intensity of the 3553.8, 1728.8, and 1715.8 cm^{-1} ones. The response of the product bands to matrix annealing allowed us to distinguish two sets of bands. D_I bands diminish and D_{II} bands increase after prolonged matrix annealing; the frequencies of the D_I and D_{II} bands observed in all spectral regions are collected in Table 3. The proximity of the D_I and D_{II} bands to the absorptions of the parent molecules facilitates their assignments to the perturbed vibrations of the diacetyl and water molecules.

Ab Initio Calculations. Kumpf and Damewood⁸ performed detailed theoretical study of the formaldehyde–water potential energy surface in the ground state. The authors reported various possible configurations of the formaldehyde–water complex that included three isomeric complexes in which water was hydrogen bonded to carbonyl group of HCHO molecule, one complex stabilized by the C–H \cdots O interaction, and seven configurations that favored electrostatic interactions between water and formaldehyde subunits. The three configurations with the O–H \cdots O(C) hydrogen bond were found to be more stable than the other eight configurations, however, one of the configurations stabilized by the dipole–dipole interaction (called by the authors side-by-side interaction) had relatively close energy to the hydrogen-bonded structures. The experimental results obtained for the studied α -dicarbonyl–water complexes demonstrate (as

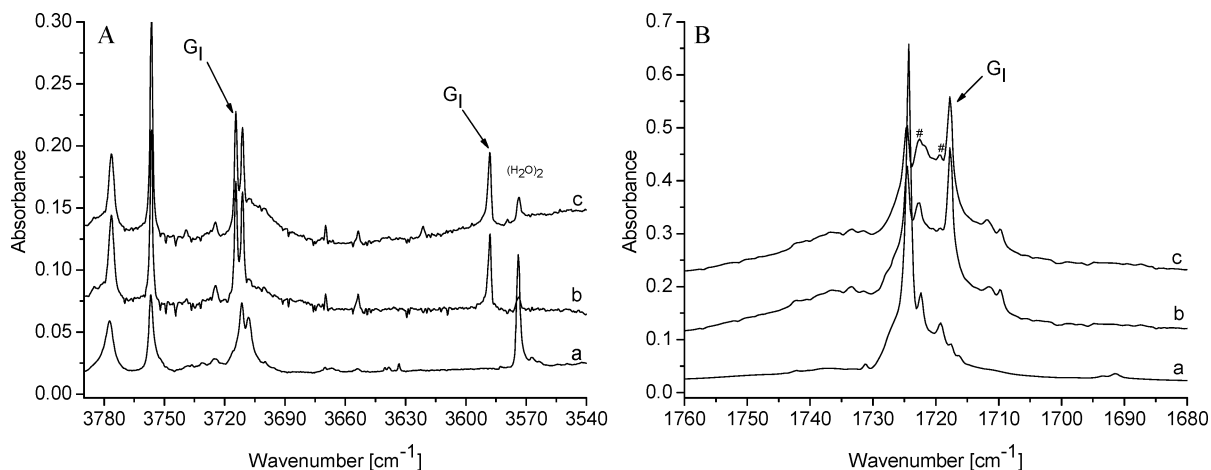


Figure 1. The $\nu(\text{OH})$ stretching region of water (A) and $\nu(\text{C}=\text{O})$ stretching region of glyoxal (B) in the spectra of matrixes: (a) $\text{H}_2\text{O}/\text{Ar} = 1/450$ (A) or $\text{CHOCHO}/\text{Ar} = 1/450$ (B), (b) $\text{CHOCHO}/\text{H}_2\text{O}/\text{Ar} = 4/2/600$, and (c) after annealing of matrix b for 10 min at 33 K. The bands marked by # are due to glyoxal dimer.

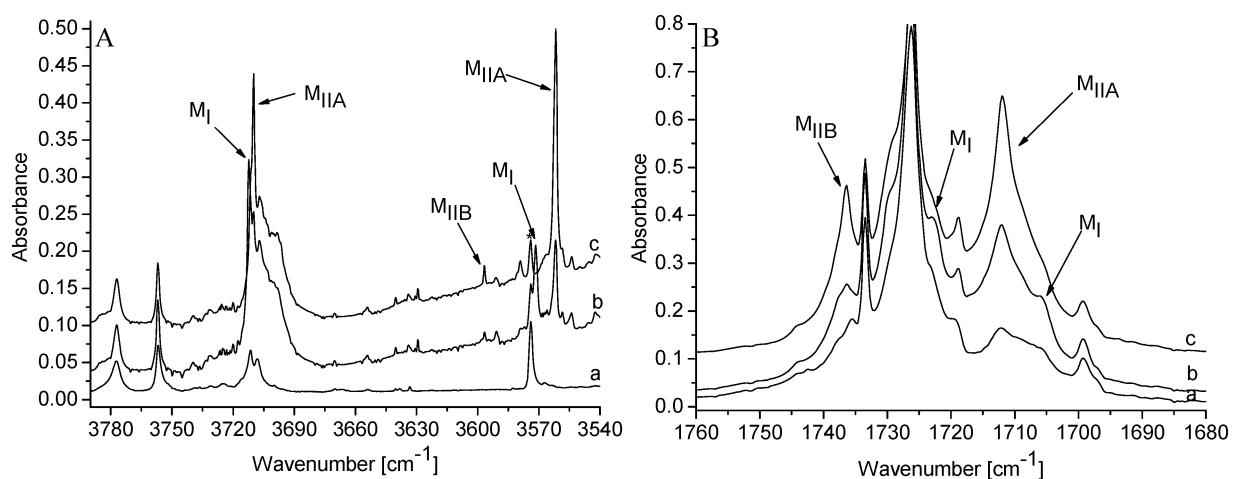


Figure 2. The $\nu(\text{OH})$ stretching region of water (A) and $\nu(\text{C}=\text{O})$ stretching region of methylglyoxal (B) in the spectra of matrixes: (a) $\text{H}_2\text{O}/\text{Ar} = 1/450$ (A) or $\text{CH}_3\text{COCHO}/\text{Ar} = 1/400$ (B), (b) $\text{CH}_3\text{COCHO}/\text{H}_2\text{O}/\text{Ar} = 3/1/1800$, and (c) after annealing of matrix b for 10 min at 33 K. The band marked by an asterisk is due to the presence of the water dimer ($\text{H}_2\text{O})_2$.

TABLE 2: The Observed Frequencies and Calculated Frequency Shifts $\Delta\nu = \nu_{\text{complex}} - \nu_{\text{monomer}}$ (cm^{-1}) and Intensities^a (km/mol) for the $\text{H}_2\text{O}\cdots\text{CH}_3\text{COCHO}$ Complexes

experimental							calculated							assignment
M^b	M_I	M_{IIA}	M_{IIB}	M_I	M_{IIA}	M_{IIB}	M^b	mIA	$mIIA$	$mIIIA$	mIK	$mIIK$	$mIIIK$	
ν	ν	ν	ν	$\Delta\nu$	$\Delta\nu$	$\Delta\nu$	ν	$\Delta\nu$	$\Delta\nu$	$\Delta\nu$	$\Delta\nu$	$\Delta\nu$	$\Delta\nu$	
2843.1	2875.2		2857.8	+32.1		+14.7	3008(61)	+16	+37	+21	+42	+2	+5	$\nu\text{C}-\text{H ald}$
2840.7	2873.0			+32.3										
1733.5	1705.3	1711.9		-28.2	-21.6		1723(36)	-5	-1	0	0	-5	-5	$\nu\text{C}=\text{O ket}$
1726.4	1722.6		1736.5	-3.8		+10.1	1720(111)	+2	-9	-5	-11	+2	+2	$\nu\text{C}=\text{O ald}$
1362.4		1367.4			+5		1376(1)	+5	+10	+6	+24	+2	+2	$\delta\text{C}-\text{H ald}$
1228.3		1240.3	1238.2		+12	+9.9	1273(17)	+1	0	0	+3	+11	+11	$\nu\text{C}-\text{C as} + \gamma\text{CH}_3$
1051.5		1053.3			+1.8		1083(3)	-1	+5	+3	+3	+2	+1	$\gamma\text{CH}_3 + \gamma\text{CH}$
777.1		782.3	785.7		+5.2	+8.6	798(13)	+1	+3	+2	+1	+3	+3	$\nu\text{C}-\text{C s}$
3735.0	3712.1	3709.9		-22.9	-25.1		3986(74)	-36	-33	-32	-38	-39	-37	νOH
3638.0	3571.5	3561.7	3596.7	-66.5	-76.3	-41.3	3865(10)	-68	-78	-64	-96	-102	-97	νOH
1590.0	1597.0	1604.0		+7	+14		1660(66)	+13	+17	+29	+17	+14	+32	δHOH

^a The intensities are given in brackets. ^b The observed and calculated frequencies of the monomers are given for comparison.

discussed further) that in the matrixes only the $\text{O}-\text{H}\cdots\text{O}(\text{C})$ hydrogen-bonded complexes are trapped. So, we focused our attention in exploring all possible structures of the α -dicarbonyls–water complexes with $\text{O}-\text{H}\cdots\text{O}(\text{C})$ hydrogen bond between water and carbonyl group.

Glyoxal–Water Complexes. Three stationary points for the $\text{Gly}\cdots\text{H}_2\text{O}$ complexes calculated at the MP2 level with the 6-311++G(2d,2p) basis set are presented in Figure 4. The

geometrical parameters that show the largest changes with respect to the isolated submolecules are presented in Table 4; the binding energies for the optimized structures are also presented. The full set of geometrical parameters for all optimized structures is available in the Supporting Information in Tables 1–3.

All three structures gI, gII, and gIII are stabilized by the hydrogen bonds. As can be seen in Figure 4, the complexes gI

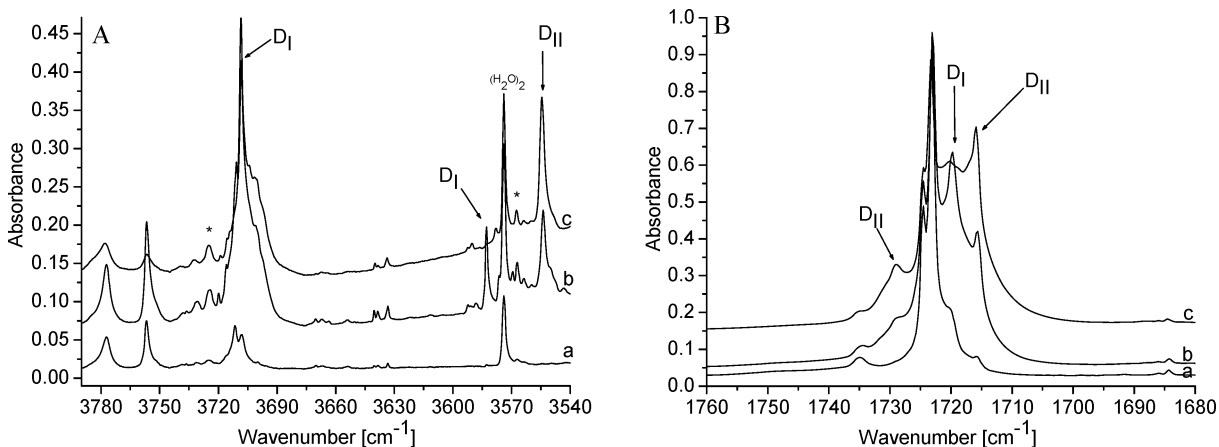


Figure 3. The $\nu(\text{OH})$ stretching region of water (A) and $\nu(\text{C}=\text{O})$ stretching region of diacetyl (B) in the spectra of matrices: (a) $\text{H}_2\text{O}/\text{Ar} = 1/450$ (A) or $\text{CH}_3\text{COCOCH}_3/\text{Ar} = 1/450$ (B), (b) $\text{CH}_3\text{COCOCH}_3/\text{H}_2\text{O}/\text{Ar} = 4/2/600$, and (c) after annealing of matrix b for 10 min at 33 K. The bands marked by asterisks are due to the presence of complex formed by nitrogen–water impurity.

TABLE 3: The Observed Frequencies and Calculated Frequency Shifts $\Delta\nu = \nu^{\text{complex}} - \nu^{\text{monomer}}$ (cm^{-1}) and Intensities^a (km/mol) for the $\text{H}_2\text{O}\cdots\text{CH}_3\text{COCOCH}_3$ Complexes

experimental					calculated				
M ^b	D _I	D _{II}	D _I	D _{II}	M ^b	d _I	d _{II}	d _{III}	assignment
ν	ν	ν	$\Delta\nu$	$\Delta\nu$	ν	$\Delta\nu$	$\Delta\nu$	$\Delta\nu$	
1723.1		1728.8		+5.7	1722(161)	0	0	0	$\nu\text{C}=\text{O}$
	1719.8	1715.8	-3.3	-7.3	1719(0)	-1	-2	-3	
					1419(0)	+3	+5	+5	δCH_3
1355.9	1356.9	1358.5	+1	+2.6	1410(56)	+1	+2	+3	
1115.0	1118.7	1122.4	+3.7	+7.4	1148(67)	+4	+7	+6	γCH_3
		1126.0		+11					
946.8	943.6	948.8	-3.2	+2	977(3)	-3	+3	+3	γCH_3
903.4		910.0		+6.6	925(23)	+6	+4	+4	$\nu\text{C}-\text{CH}_3$
900.5		906.0		+5.5					
3735.0		3708.3		-26.7	3986(74)	-38	-39	-38	νOH
3638.0	3582.8	3553.8	-55.2	-84.2	3865(10)	-82	-110	-105	νOH
1590.0	1606.0	1606.0	+16	+16	1660(66)	+17	+17	+33	δHOH

^a The intensities are given in brackets. ^b The observed and calculated frequencies of the monomers are given for comparison.

and gII adopt ringlike configurations in which one of the water hydrogens forms $\text{O}-\text{H}\cdots\text{O}(\text{C})$ hydrogen bond with an oxygen atom of one of the CHO groups while the water oxygen points toward the hydrogen atom of the same or the other CHO group (structures II and I, respectively). The $\text{O}-\text{H}\cdots\text{O}(\text{C})$ bond is manifested by lengthening of the OH and C=O bonds in the two structures (by ca. 0.005 Å for the O–H and by ca. 0.003 Å for the C=O bond). The length of the $(\text{O})\text{H}\cdots\text{O}(\text{C})$ bond is very similar in the two complexes (2.04 and 2.06 Å in gI and gII, respectively) suggesting hydrogen bond of similar strength. The obtained geometrical parameters suggest also weak $\text{C}-\text{H}\cdots\text{O}(\text{H}_2)$ interactions in the complexes gI and gII; the interaction is slightly stronger in the structure gI than in gII as demonstrated by shorter $(\text{C})\text{H}\cdots\text{O}(\text{H}_2)$ distance in gI (2.385 Å in gI as compared with 2.587 Å in gII). In both structures, the $\text{C}-\text{H}\cdots\text{O}(\text{H}_2)$ interaction leads to the shortening of the C–H bond (by 0.003 Å both in gI and gII) indicating that weak, improper hydrogen bond is formed. The formation of the improper hydrogen bonds by the C–H proton donors is nowadays a well-known phenomena.^{49,50} The configuration gI is the most stable one, however, all the three configurations gI, gII, and gIII have close binding energies ($\Delta E^{\text{CP}}(\text{ZPE}) = -2.60, -2.31, \text{ and } -1.98$ kcal/mol for gI, gII, and gIII, respectively). In configuration gIII, the water molecule is slightly reoriented from its position in configuration gI in such a way that the $\text{O}-\text{H}\cdots\text{O}(\text{C})$ interaction is favored and the $\text{C}-\text{H}\cdots\text{O}(\text{H}_2)$ interaction is disrupted. This is reflected in shorter $(\text{O})\text{H}\cdots\text{O}(\text{C})$ and longer $(\text{C})\text{H}\cdots\text{O}(\text{H}_2)$ distance in configuration gIII as

compared to gI (1.98, 2.78 Å; 2.04, 2.38 Å in structures gIII, gI, respectively); the $\text{O}-\text{H}\cdots\text{O}$ angle increases from 149.8° in gI to 176.7° in gIII. The disruption of the $\text{C}-\text{H}\cdots\text{O}(\text{H}_2)$ interaction in gIII is responsible for the lower stability of this complex as compared to the gI one. As part of our configurational search, we were looking for hydrogen-bonded configuration (corresponding to 1c in Kumpf and Damewood paper) in which the lone pairs of the carbonyl oxygen form a bifurcated arrangement with one of the water hydrogens leading to linear $\text{C}=\text{O}\cdots\text{H}-\text{O}$ arrangement. However, such a linear arrangement of the interacting C=O and O–H groups corresponded to saddle point on the potential energy surface ($\Delta E^{\text{CP}}(\text{ZPE}) = -1.30$ kcal/mol) and not to a local minimum. The relative stability ordering for the configurations considered in this study obtained at the MP2/6-31++G(2d,2p) level is gI > gII > gIII.

In Table 1, the observed frequencies of the $\text{Gly}\cdots\text{H}_2\text{O}$ complex trapped in solid argon are compared with the calculated ones for the optimized configurations. The whole set of calculated frequencies for the three configurations is presented in the Supporting Information in Table 4. The calculations resulted in a similar set of frequencies for the three configurations stabilized by the hydrogen bonding. The formation of the $\text{O}-\text{H}\cdots\text{O}(\text{C})$ bond is reflected by the red shifts of the water OH and glyoxal C=O stretching frequencies after complex formation ($-76, -67, \text{ and } -74$ cm^{-1} for the OH stretch and $-9, -5, \text{ and } -5$ cm^{-1} for the C=O stretch in structures gI, gII, and gIII, respectively). In turn, the $\text{C}-\text{H}\cdots\text{O}(\text{H}_2)$ interaction leads to a noticeable blue shift of the activated CH stretching

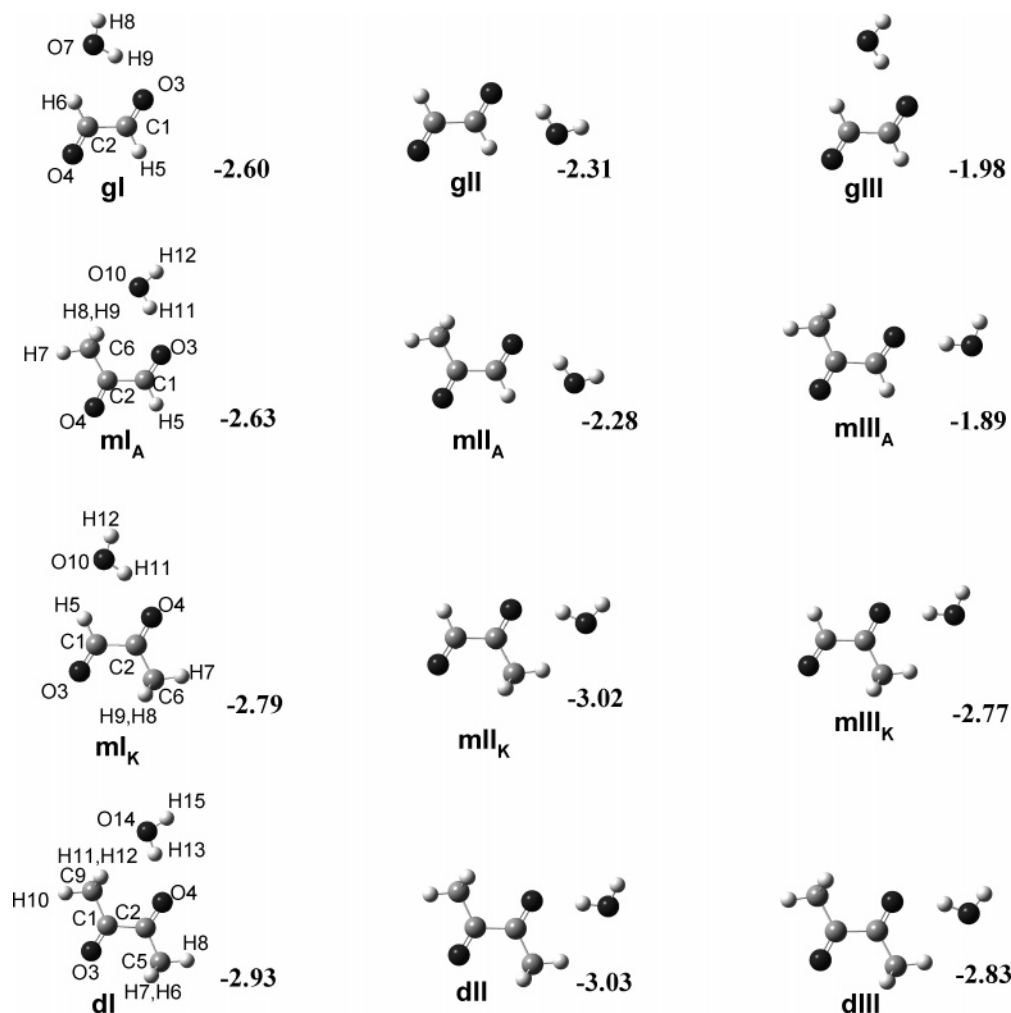


Figure 4. The optimized structures of α -dicarbonyls with water. Binding energies ΔE^{CP} (ZPE) are given in kcal/mol.

TABLE 4: Calculated Properties^a of the $\text{H}_2\text{O}\cdots\text{CHOCHO}$ Complexes^b

property	monomers	gI	gII	gIII
$r(\text{C}_1\text{--C}_2)$	1.518	1.520	1.517	1.519
$r(\text{C}_1\text{=O}_3)$	1.215	1.218	1.219	1.218
$r(\text{C}_1\text{--H}_5)$	1.100	1.099	1.097	1.098
$r(\text{C}_2\text{=O}_4)$	1.215	1.217	1.215	1.216
$r(\text{C}_2\text{--H}_6)$	1.100	1.097	1.100	1.099
$r(\text{H}_9\text{--O}_7)$	0.958	0.964	0.963	0.963
$r(\text{O}_7\text{--H}_8)$	0.958	0.958	0.957	0.958
$R(\text{H}_9\cdots\text{O}_3)$		2.041	2.062	1.981
$R(\text{O}_7\cdots\text{H}_5)$			2.587	
$R(\text{O}_7\cdots\text{H}_6)$		2.385		2.780
$\Theta(\text{C}_1\text{O}_3\text{H}_9)$		116.1	99.67	117.4
$\Theta(\text{O}_3\text{H}_9\text{O}_7)$		149.8	141.47	176.7
ΔE^{CP}		-4.34	-3.94	-3.57
ΔE^{CP} (ZPE)		-2.60	-2.31	-1.98

^a Bond lengths in Å, angles in degrees, energies in kcal/mol. ^b The corresponding parameters of monomers are given for comparison.

frequencies in the complexes gI and gII (+45, +36 cm^{-1}); in complex gIII, the corresponding vibration is less perturbed because of the lack of the $\text{C}\text{--H}\cdots\text{O}(\text{H}_2)$ interaction in this complex.

Methylglyoxal–Water Complexes. Six stationary points for the $\text{MGly}\cdots\text{H}_2\text{O}$ complexes calculated at the MP2 level with the 6-311++G(2d,2p) basis set are presented in Figure 4; the selected geometrical parameters are collected in Table 5. The structures mI_A , mII_A , and mIII_A describe the hydrogen-bonded

complexes with water attached to the carbonyl oxygen of the aldehyde group, and the structures mI_K , mII_K , and mIII_K correspond to the hydrogen-bonded complexes with water bonded to the carbonyl oxygen of the keto group.

The structures mI_A and mII_A show great similarities to the structures gI and gII of $\text{Gly}\text{--H}_2\text{O}$ complexes. Similarly, like the structures gI and gII, they adopt ringlike configurations with the $\text{O}\text{--H}\cdots\text{O}(\text{C})$ hydrogen bond and, possibly, with a very weak $\text{C}\text{--H}\cdots\text{O}(\text{H}_2)$ interaction. The $(\text{O})\text{H}\cdots\text{O}(\text{C})$ bond lengths in the structures mI_A and mII_A are equal to 2.00 Å and 2.03 Å, as compared with 2.04 and 2.06 Å for the $(\text{O})\text{H}\cdots\text{O}(\text{C})$ bond lengths in complexes gI and gII. In turn, the $(\text{C})\text{H}\cdots\text{O}(\text{H}_2)$ distances in mI_A and mII_A are equal to 2.60 Å and 2.66 Å as compared to 2.38 and 2.59 Å in gI and gII. The noticeably shorter distance between one of the three hydrogen atoms of the methyl group and water oxygen (2.601 Å versus 2.917) in mI_A suggests a weak interaction between this hydrogen and the oxygen atom of water. It is interesting to note very close values of the binding energies for the structures gI and mI_A (ΔE^{CP} (ZPE) = -2.60 and -2.63 kcal/mol) and gII and mII_A (ΔE^{CP} (ZPE) = -2.31 and -2.28 kcal/mol, respectively). In the configuration mIII_A , the water is slightly reoriented from its position in configuration mII_A in such a way that the $\text{O}\text{--H}\cdots\text{O}(\text{C})$ bond is directed along one of the lone electron pairs of carbonyl oxygen atom which leads to disruption of the weak $\text{C}\text{--H}\cdots\text{O}(\text{H}_2)$ bond and less stability of the mIII_A structure with respect to mII_A one (ΔE^{CP} (ZPE) = -1.89 kcal/mol).

TABLE 5: Calculated Properties^a of the $\text{H}_2\text{O}\cdots\text{CH}_3\text{COCHO}$ Complexes^b

property	monomers	mI _A	mII _A	mIII _A	mI _K	mII _K	mIII _K
$r(\text{C}_1\text{--C}_2)$	1.528	1.529	1.526	1.526	1.530	1.528	1.527
$r(\text{C}_1\text{=O}_3)$	1.215	1.217	1.219	1.218	1.217	1.214	1.214
$r(\text{C}_1\text{--H}_5)$	1.101	1.100	1.098	1.099	1.098	1.101	1.100
$r(\text{C}_2\text{=O}_4)$	1.221	1.222	1.221	1.220	1.225	1.225	1.225
$r(\text{C}_2\text{--C}_6)$	1.498	1.495	1.498	1.498	1.496	1.494	1.495
$r(\text{C}_6\text{--H}_7)$	1.083	1.083	1.083	1.083	1.083	1.083	1.084
$r(\text{C}_6\text{--H}_8)$	1.088	1.088	1.088	1.088	1.088	1.088	1.088
$r(\text{C}_6\text{--H}_9)$	1.088	1.088	1.088	1.088	1.088	1.088	1.088
$r(\text{H}_{11}\text{--O}_{10})$	0.958	0.963	0.964	0.963	0.965	0.965	0.965
$r(\text{O}_{10}\text{--H}_{12})$	0.958	0.958	0.957	0.957	0.958	0.958	0.957
$R(\text{H}_{11}\cdots\text{O}_3)$		1.999	2.029	2.010			
$R(\text{H}_{11}\cdots\text{O}_4)$					1.993	1.981	1.950
$R(\text{O}_{10}\cdots\text{H}_5)$			2.657	3.647	2.421		
$R(\text{O}_{10}\cdots\text{H}_7)$						2.448	2.818
$R(\text{O}_{10}\cdots\text{H}_8)$		2.601					
$R(\text{O}_{10}\cdots\text{H}_9)$		2.917					
$\Theta(\text{C}_1\text{O}_3\text{H}_{11})$		133.5	100.6	117.4			
$\Theta(\text{C}_2\text{O}_4\text{H}_{11})$					119.3	114.5	117.7
$\Theta(\text{O}_3\text{H}_{11}\text{O}_{10})$		165.1	146.0	176.7			
$\Theta(\text{O}_4\text{H}_{11}\text{O}_{10})$					155.63	158.25	176.7
ΔE^{CP}		-4.33	-3.90	-3.27	-4.53	-4.72	-4.31
ΔE^{CP} (ZPE)		-2.63	-2.28	-1.89	-2.79	-3.02	-2.77

^a Bond lengths in Å, angles in degrees, energies in kcal/mol. ^b The corresponding parameters of monomers are given for comparison.

The configurations with water attached to the keto group of methylglyoxal mI_K, mII_K, and mIII_K are more stable than the three corresponding configurations with water attached to the aldehyde group. The mI_K and mII_K structures are stabilized mainly by the O–H \cdots O(C) hydrogen bond. However, like in the mI_A and mII_A configurations, there is probably a very weak C–H \cdots O(H₂) interaction in these two complexes. The calculated shortening of the CH bond of the MGly aldehyde group by 0.003 Å after mI_K formation suggests formation of an improper hydrogen bonding by CH group in mI_K. The relatively short distance between the water oxygen and one of the three hydrogen atoms of the CH₃ group in mII_K (2.448 Å) suggests the C–H \cdots O(H₂) interaction. The two complexes, mI_K and mII_K, have very close values of the binding energies (ΔE^{CP} (ZPE) = -2.79 and -3.02 kcal/mol). In the configuration mIII_K like in mIII_A, water is slightly reoriented from its position in mII_K and the structure is stabilized by the O–H \cdots O(C) interaction only. This configuration is slightly less stable than the mII_K one (ΔE^{CP} (ZPE) = -2.77 kcal/mol).

Similarly, like in the case of glyoxal complexes, a linear arrangement of the C=O and O–H groups corresponds to saddle points on the potential energy surface (ΔE^{CP} (ZPE) = -1.61 and -1.73 kcal/mol when water is attached to aldehyde and keto groups, respectively).

The relative stability ordering for the methylglyoxal–water complexes mII_K > mI_K \cong mIII_K \cong mI_A > mII_A > mIII_A clearly shows that the complexes with water attached to the keto group are more stable than the complexes with water attached to the aldehyde group.

The six optimized MGly \cdots H₂O structures are characterized by similar sets of frequencies (see Table 2 and Table 5 in Supporting Information). The largest frequency differences between various configurations are calculated for the groups that are involved in the O–H \cdots O(C) and/or C–H \cdots O(H₂) hydrogen bonding. So, the C–H stretching vibrations of the CHO groups exhibit the largest perturbation from MGly monomer value in the mI_K and mII_A configurations (+42 and +37 cm⁻¹, respectively) in which the hydrogen atom of the CHO group interacts with the water oxygen. The blue shift of the CH stretching frequencies is in accord with the CH bond shortening and confirms the formation of the improper hydrogen

bonding. The perturbation of the C–H stretching vibration in mI_K and mII_A is accompanied by the noticeable perturbation of the C–H deformation vibration (+24 and +10 cm⁻¹ in mI_K and mII_A, respectively). The O–H \cdots O(C) interaction affects the aldehyde or keto C=O stretching vibrations (that are coupled with water bending vibration) and the OH stretching vibration of water. The three configurations (mI_A, mII_K, and mIII_K) exhibit the same perturbations of the keto C=O and aldehyde C=O stretching vibrations (see Table 2). In turn, in the mI_K and mII_A structures, the C=O stretching vibrations of the aldehyde and keto groups also exhibit very similar perturbations; the C=O stretching frequency of the CHO group is calculated to shift -11 and -9 cm⁻¹ from the corresponding MGly frequency in mI_K and mII_A, respectively, whereas the keto C=O stretches exhibit negligible perturbation. The calculations predict similar perturbations of the OH vibrations in mI_K, mII_K, and mIII_K configurations (-96, -102, and -97 cm⁻¹, respectively) that are larger than those in mI_A, mII_A, and mIII_A structures (-68, -78, and -64 cm⁻¹, respectively).

Diacetyl–Water Complexes Three stationary points for the DAc \cdots H₂O complexes calculated at the MP2 level with the 6-311++G(2d,2p) basis set are presented in Figure 4; the selected geometrical parameters are collected in Table 6.

The dI, dII, and dIII structures of diacetyl show great similarities to the mI_K, mII_K, and mIII_K structures of methylglyoxal. The dI and dII complexes, similarly to the mI_K and mII_K ones, are stabilized by the O–H \cdots O(C) bond; in dII, there is possibly also a very weak C–H \cdots O(H₂) interaction (between water oxygen atom and one of the hydrogen atoms of the CH₃ group). The (C)H \cdots O(H₂) distance between the water oxygen and one of the three hydrogen atoms of CH₃ is almost the same in dII and in mII_K (2.478 and 2.448 Å, respectively). In the configuration dIII, the water is slightly reoriented from its position in dII, the (C)H \cdots O(H₂) distance increases to 2.77 Å, and the structure is stabilized by the O–H \cdots O(C) interaction only (like in the structure mIII_K with respect to mII_K). All three configurations are characterized by close binding energies (ΔE^{CP} (ZPE) = -2.93, -3.03, and -2.83 kcal/mol for dI, dII, and dIII, respectively).

There are very small differences between the calculated frequencies of the three optimized structures.

TABLE 6: Calculated Properties^a of the H₂O⋯CH₃COCOCH₃ Complexes^b

property	monomers	dI	dII	dIII
$r(C_1-C_2)$	1.540	1.542	1.541	1.540
$r(C_1=O_3)$	1.221	1.221	1.220	1.220
$r(C_1-C_9)$	1.501	1.497	1.501	1.500
$r(C_2=O_4)$	1.221	1.223	1.225	1.225
$r(C_2-C_5)$	1.501	1.498	1.496	1.497
$r(C_5-H_6)$	1.088	1.088	1.088	1.088
$r(C_5-H_7)$	1.087	1.087	1.088	1.088
$r(C_5-H_8)$	1.083	1.083	1.083	1.084
$r(C_9-H_{10})$	1.083	1.083	1.083	1.083
$r(C_9-H_{11})$	1.088	1.088	1.087	1.088
$r(C_9-H_{12})$	1.087	1.088	1.088	1.088
$r(H_{13}-O_{14})$	0.958	0.964	0.966	0.965
$r(O_{14}-H_{15})$	0.958	0.958	0.958	0.957
$R(H_{13}\cdots O_4)$		1.963	1.965	1.945
$R(O_{14}\cdots H_8)$			2.478	2.775
$R(O_{14}\cdots H_{11})$		2.805		
$R(O_{14}\cdots H_{12})$		2.704		
$\Theta(C_2O_4H_{13})$		137.7	115.2	117.4
$\Theta(O_4H_{13}O_{14})$		169.4	160.8	176.7
ΔE^{CP}		-4.67	-4.74	-4.44
$\Delta E_{CP}(ZPE)$		-2.93	-3.03	-3.21

^a Bond lengths in Å, angles in degrees, energies in kcal/mol. ^b The corresponding parameters of monomers are given for comparison.

Discussion

Glyoxal–Water Complexes. The spectra of Gly/H₂O/Ar matrixes evidence the presence of one complex in the studied matrixes. The relatively large red shift of the two water OH stretching frequencies (-20.7 and -49.4 cm⁻¹) and the observed red shift of the C=O stretching frequency of glyoxal (-6.6 cm⁻¹) indicate that in the matrix is trapped the hydrogen-bonded complex with the water molecule attached to the carbonyl group of glyoxal. The calculations indicate the stability of three different configurations of hydrogen-bonded complex, however, their spectroscopic characteristics are very similar (see Table 1) and do not allow us to conclude which of the three configurations is trapped in the matrix. It seems reasonable to assume that the most stable complex gI is present in the matrix. The trapping of the most stable complex corresponding to global minimum on potential energy surface suggests very small transition barrier between various stable configurations.

Methylglyoxal–Water Complexes. The spectra of MGly/H₂O/Ar matrixes evidence the presence of three MGly–water complexes in the studied matrixes that are characterized by the M_I, M_{IIA}, and M_{IIIB} band sets. The M_I bands disappear whereas the M_{IIA} and M_{IIIB} bands increase after matrix annealing. The most informative, as far as the structures of the complexes are concerned, are the bands identified for the C–H, C=O, and O–H stretching vibrations. The M_I group involves the 2875.2, 2873.0 cm⁻¹ and the 1722.6, 1705.3 cm⁻¹ bands in the C–H and C=O stretching regions, respectively, and the 3571.5 cm⁻¹ absorption because of perturbed water vibration. The 2875.2 and 2873.0 cm⁻¹ bands are ca. 32 cm⁻¹ blue-shifted from the MGly monomer frequency which suggests that they are due to the mI_K or mII_A complexes. The other configurations do not exhibit such a large perturbation of the C–H stretching vibration (see Table 2). The observed C=O stretches are -3.8 and -28.2 cm⁻¹ shifted from their MGly monomer values which are in fair agreement with the spectroscopic characteristics of the mI_K and mII_A structures. Careful analysis of the perturbed water stretching vibrations allows us to assign the M_I bands to the mI_K structure. The two perturbed OH stretching vibrations observed at 3561.7 and 3571.5 cm⁻¹ exhibit similar red shifts

(-76.3 and -66.5 cm⁻¹) whereas the 3596.7 cm⁻¹ band is noticeably less shifted (-41.3 cm⁻¹) from the water monomer vibration at 3638 cm⁻¹. This suggests that the 3561.7 and 3571.5 cm⁻¹ bands correspond to complexes in which water is bonded to the keto group whereas the 3596.7 cm⁻¹ band corresponds to complex with water attached to the aldehyde group. The calculations show that in mI_K, mII_K, and mIII_K complexes the OH stretching vibration is characterized by similar frequency values that are noticeably lower than those for mI_A, mII_A, and mIII_A structures. So, we assigned the M_I bands to mI_K structure. The frequencies of the other identified M_I vibrations (see Table 2) are in accord with the calculated ones for the mI_K structure. The strong decrease of the M_I bands after annealing (and disappearance after prolonged annealing) may be explained by the conversion of the less stable mI_K configuration to the slightly more stable mII_K one. Indeed, the M_{IIA} bands that are strongly growing after matrix annealing are assigned with confidence to the mII_K structure. As already was mentioned, the 3561.7 cm⁻¹ M_{IIA} band due to the OH stretching is attributed to one of the other two complexes, mII_K or mIII_K, with H₂O bonded to the keto group of methylglyoxal. We assigned the M_{IIA} band set to mII_K complex which is predicted to be slightly more stable than the mI_K and mIII_K complexes. This explains the increase of the M_{IIA} bands at the expense of the M_I ones after matrix annealing as because of conversion of the less stable mI_K configuration into the more stable mII_K one. The mII_K and mIII_K structures show large similarity and are characterized by very similar sets of frequencies, so, the larger stability of the mII_K (than the mI_K one) is the only criterion for differentiation between the two structures. The M_{IIIB} bands are assigned to mI_A complex, the most stable among the three optimized complexes with H₂O attached to the aldehyde group. Two bands belonging to M_{IIIB} group, namely, the band at 2857.8 cm⁻¹ because of C–H stretch and the 3596.7 cm⁻¹ band because of O–H stretch, evidence that M_{IIIB} bands are due to mI_A complex. The 3596.7 cm⁻¹ band is 41.3 cm⁻¹ red-shifted from the corresponding H₂O vibration which suggests that the band is due to a complex with water attached to aldehyde C=O group. The 14.7 cm⁻¹ blue shift of the CH stretching frequency from its value in MGly monomer is consistent with the shift calculated for the mI_A complex; the shifts predicted for the two other optimized mII_A and mIII_A structures are larger and, moreover, they are less stable than the mI_A configuration.

Diacetyl–Water Complexes. The spectra of DAc/H₂O/Ar matrixes clearly show that two isomeric structures of DAc⋯H₂O complex are trapped in the matrix. As discussed below, the comparison of the experimental frequencies of the D_I and D_{II} band sets with the calculated frequencies for the three optimized structures dI, dII, and dIII suggests that the D_I band set corresponds to the structure dI whereas the D_{II} band set belongs to the structure dII. The 3553.8 cm⁻¹ D_{II} band due to the perturbed OH stretching vibration of water molecule is 29 cm⁻¹ red-shifted with respect to the corresponding 3582.8 cm⁻¹ D_I band in accord with the calculated frequency shift for the dII OH stretching vibration with respect to dI one (28 cm⁻¹, see Table 3). One of the γ CH₃ rocking vibrations is calculated to shift toward lower frequencies in dI and toward higher frequencies in dII with respect to DAc monomer as observed for the 943.6 and 948.8 cm⁻¹ experimental frequencies belonging to D_I and D_{II}. As can be seen in Figure 4, the conversion between the complexes dI and dII may occur by the rotation of H₂O molecule with respect to diacetyl without disruption of the O–H⋯O(C) bond, so the barrier for the conversion is expected to be small. This fact and the slightly larger stability

of dII with respect to dI may be the reason why matrix annealing leads to conversion of dI into dII.

Hydrogen Bonding in the Complexes of Glyoxal, Methylglyoxal, and Diacetyl with Water. The calculations show, in accord with earlier experimental and theoretical results, that the carbonyl oxygen of the keto group is a stronger proton acceptor than the carbonyl oxygen of the aldehyde group. This is best demonstrated by comparing the binding energies of the gIII and mIII_A complexes ($\Delta E^{\text{CP}}(\text{ZPE}) = -1.98$ and -1.89 kcal/mol) that are stabilized by the O–H \cdots O(CH) bond with the binding energies of the mIII_K and dIII ones ($\Delta E^{\text{CP}}(\text{ZPE}) = -2.77$ and -2.83 kcal/mol) stabilized by the O–H \cdots O(CH₃) bond. The above complexes are stabilized by one hydrogen bonding only. The presence of the second weak C–H \cdots O interaction between the aldehyde CH bond or one of the methyl C–H bonds and water oxygen increases the complex stability. The gI and mI_A complexes stabilized by both the C–H \cdots O and O–H \cdots O interaction have binding energy values ($\Delta E^{\text{CP}}(\text{ZPE}) = -2.60$ and -2.63 kcal/mol) close to the value characteristic for the mIII_K complex (-2.77 kcal/mol) that is stabilized by the O–H \cdots O(CCH₃) bond only. The replacement of the aldehyde group hydrogen in glyoxal by the methyl group in methylglyoxal only slightly affects the interaction energy of the complexes stabilized by the O–H \cdots O(CH) bond. The gI complex has very close binding energy value to the mI_A complex ($\Delta E^{\text{CP}}(\text{ZPE}) = -2.60$ and -2.63 kcal/mol for gI and mI_A), and the gII complex has very close binding energy value to mII_A one (-2.31 and -2.28 kcal/mol for mI_A and mII_A). Similarly, the replacement of the aldehyde group hydrogen in methylglyoxal by methyl group in diacetyl has negligible effect on the complexes stabilized by the O–H \cdots O(CCH₃) bond. The mI_K and dI complexes are characterized by very close binding energies (-2.79 and -2.93 kcal/mol) similarly to the mII_K and dII ones (-3.02 and -3.03 kcal/mol).

The interaction of the C–H bond of CHO group with water oxygen in gI, gII, mII_A, and mI_K complexes leads to the formation of the improper hydrogen bonding characterized by the shortening of the C–H bond with accompanied blue shift of the CH stretching frequency. The calculations result in the C–H bond shortening by ca. 0.003 Å in the four complexes. The calculated C–H stretching frequencies are 45, 13 cm⁻¹ and 36, 3 cm⁻¹ blue-shifted from glyoxal monomer values in gI and gII complexes, 37 cm⁻¹ in mII_A complex, and 42 cm⁻¹ in mI_K. We have identified in the matrix one glyoxal complex (most probably gI one), and the C–H stretching frequency identified for this complex was 2.5 cm⁻¹ blue-shifted with respect to the C–H stretch of glyoxal, so, the observed shift was much smaller than that of the calculated ones. For the mI_K complex, the observed CH stretching frequency is 32 cm⁻¹ blue-shifted from the corresponding frequency of methylglyoxal monomer which is in good agreement with the calculated value (42 cm⁻¹). The mII_A complex has not been identified in the studied matrixes.

The calculated geometrical parameters (CH \cdots O(H₂) bond lengths) and interaction energies for the mI_A, mII_K, dI, and dII complexes suggest that in these four complexes there exists a very weak interaction between hydrogen atoms of methyl group and the oxygen atom of the water molecule. The relatively short (H₂C)H \cdots O(H₂) distances in the mII_K, dII, and mI_A complexes (2.448, 2.478, and 2.601 Å, respectively) between one of the hydrogen atoms of the CH₃ group and water oxygen suggest an interaction of the water oxygen with one hydrogen atom of the CH₃ group. In dI configuration, two (H₂)CH \cdots O(H₂) lengths have comparable values (2.805, 2.703 Å) which may indicate

double interaction, however, the two distances are longer than for the mII_K, dII, and mI_A complexes, and it is hard to draw conclusion whether there is an interaction in this case. Unfortunately, the CH₃ stretching vibrations were not identified for these four complexes.

Recently, Karpfen and Kryachko⁵¹ in a series of computational papers showed that the blue shifts of the C–H stretching frequencies upon complex formation with an interacting partner may be due to so-called negative intramolecular coupling between the C–H bonds and the vicinal bonds. If the vicinal bonds stretch upon complex formation, the negative coupling causes a shortening of the C–H bonds; this effect the authors term as “negative intramolecular response” (NIR). Although we cannot exclude the NIR effect in some of the studied α -dicarbonyl–water complexes, this effect does not explain the properties of the studied complexes. First, in the gI, mI_A, mI_K, and dI complexes, the water molecule forms the O–H \cdots O hydrogen bond with a carbonyl oxygen of one CHO or C(CH₃)O group and a weak improper O \cdots H–C hydrogen bond with the C–H bond of the other CHO or C(CH₃)O group of α -dicarbonyl molecule. The effect of the O–H \cdots O bond formation by one CHO/C(CH₃)O group on the geometry of the other CHO/C(CH₃)O group is very small as indicated by the geometrical parameters of the gII, mII_A, mIII_A, mII_K, mIII_K, dII, and dIII complexes (see Tables 4–6 and Tables 1–3 in Supporting Information). Second, the NIR effect does not explain the energy difference in the mII_A, mIII_A and mII_K, mIII_K pairs of complexes. Small reorientation of H₂O with respect to carbonyl oxygen in the mII_A and mII_K complexes leading to the rupture of the postulated C–H \cdots O interaction is followed by the decrease of the binding energy of the mIII_A and mIII_K complexes with respect to the mII_A and mII_K ones (see Figure 4). A weak C–H \cdots O interaction between C–H group and water oxygen in mII_A, mII_K, and dII complexes explains the larger stability of these complexes.

Conclusions

Matrix-isolation FTIR spectroscopy has been applied to study the complexes formed by three atmospheric α -dicarbonyls: glyoxal, methylglyoxal, and diacetyl with the water molecule. The spectra analysis evidenced the presence of one Gly \cdots H₂O complex, three MGly \cdots H₂O complexes, and two DAC \cdots H₂O ones in the studied matrixes. The strong perturbation of the water-stretching vibration indicates that all complexes are stabilized by the O–H \cdots O(C) hydrogen bonding with the OH group of water attached to the carbonyl oxygen of the aldehyde group or to the keto group.

Theoretical study performed at the MP2/6-311++G(2d,2p) level indicated the stability of three Gly \cdots H₂O complexes (gI, gII, gIII), six MGly \cdots H₂O complexes (mI_A, mII_A, mIII_A, mI_K, mII_K, and mIII_K), and three DAC \cdots H₂O ones (dI, dII, dIII) that are stabilized by the O–H \cdots O(C) hydrogen bonding with the OH group of water attached to the carbonyl oxygen of the aldehyde group (gI, mI_A) or the keto group (mI_K, mII_K, dI, dII). Moreover, the calculated geometrical parameters and vibrational frequencies suggest that in the gI, gII, mII_A, and mI_K complexes there is additionally a weak C–H \cdots O(H₂) interaction between the water oxygen and CH aldehyde group whereas in mI_A, mII_K, dI, and dII exists still weaker interaction between one of the hydrogens of the methyl group and water. The comparison of the theoretical and experimental frequencies allowed us to attribute tentatively the structures mI_A, mI_K, and mII_K to the three MGly \cdots H₂O complexes present in the matrixes and the specific structures dI and dII to the two DAC \cdots H₂O complexes.

The blue shift of the CH stretching frequencies upon complex formation observed in the spectra of the Gly \cdots H $_2$ O complex and in two MGly \cdots H $_2$ O complexes present in matrixes matches well the calculated CH length shortening and evidences the existence of improper C–H \cdots O hydrogen bonding in these three complexes.

Both the calculated properties (binding energies, geometrical parameters, and vibrational frequencies) and experimental spectra evidence that the keto group is a stronger proton acceptor than the carbonyl oxygen of the aldehyde group.

Acknowledgment. We gratefully acknowledge a grant of computer time from the Wrocław Center for Networking and Supercomputing (WCSS).

Supporting Information Available: Geometrical parameters, vibrational frequencies, and intensities of the CHOCHO, CH $_3$ COCHO, CH $_3$ COCOCH $_3$, and H $_2$ O monomers and H $_2$ O \cdots CHOCHO, H $_2$ O \cdots CH $_3$ COCHO, and H $_2$ O \cdots CH $_3$ -COCOCH $_3$ complexes calculated at the MP2/6-311++G-(2d,2p) level. This material is available free of charge via the Internet at <http://pubs.acs.org>.

References and Notes

- (1) Finlayson-Pitts, B. J.; Pitts, J. N., Jr. *Atmospheric Chemistry*; Wiley: New York, 1986.
- (2) Aloisio, S.; Francisco, J. S. *Phys. Chem. Earth C* **2000**, *25*, 245.
- (3) McKeen, S. A.; Gierczak, T.; Burkholder, J. B.; Wennberg, P. O.; Hanisco, T. F.; Keim, E. R.; Gao, R.-S.; Liu, S. C.; Ravishankara, A. R.; Fahey, D. W. *Geophys. Res. Lett.* **1997**, *24*, 3177.
- (4) Klotz, B.; Graedler, F.; Sørensen, S.; Barnes, I.; Becker, K. H. *Int. J. Chem. Kinet.* **2001**, *3*, 39.
- (5) Munger, J. W.; Jacob, D. J.; Walkman, J. M.; Hoffman, M. R. *J. Geophys. Res.* **1983**, *88*, 5109.
- (6) Fung, K.; Grosjean, D. *Anal. Chem.* **1981**, *53*, 168.
- (7) Ventura, O. N.; Coitino, E. L.; Lledos, A.; Bertran, J. *J. Comput. Chem.* **1992**, *13*, 1037.
- (8) Kumpf, R. A.; Damewood, J. R., Jr. *J. Phys. Chem.* **1989**, *93*, 4478.
- (9) Ventura, O. N.; Coitino, E. L.; Irving, K.; Iglesias, A.; Lledos, A. *J. Mol. Struct. (THEOCHEM)* **1990**, *210*, 427.
- (10) Lewell, X. O.; Hillier, I. H.; Field, M. J.; Morris, J. J.; Taylor, P. *J. J. Chem. Soc., Faraday Trans. 2* **1988**, *84*, 893.
- (11) Blair, J. T.; Westbrook, J. D.; Levy, R. M.; Krogh-Jespersen, K. *Chem. Phys. Lett.* **1989**, *154*, 531.
- (12) Blair, J. T.; Krogh-Jespersen, K.; Levy, R. M. *J. Am. Chem. Soc.* **1989**, *111*, 6948.
- (13) Fukunaga, H.; Morokuma, K. *J. Phys. Chem.* **1993**, *97*, 59.
- (14) Dimitrova, Y.; Peyerimhoff, S. D. *Z. Phys. D* **1994**, *32*, 241.
- (15) Dimitrova, Y.; Peyerimhoff, S. D. *Chem. Phys. Lett.* **1994**, *227*, 384.
- (16) Dimitrova, Y. *J. Mol. Struct. (THEOCHEM)* **1997**, *391*, 251.
- (17) Sanchez, M. L.; Aguilar, M. A.; Olivares del Valle, F. J. *J. Phys. Chem.* **1995**, *99*, 15758.
- (18) Morokuma, K. *J. Chem. Phys.* **1971**, *55*, 1236.
- (19) Butler, L. G.; Brown, T. L. *J. Am. Chem. Soc.* **1981**, *103*, 6541.
- (20) Del Bene, J. E. *J. Am. Chem. Soc.* **1973**, *95*, 6517.
- (21) Ramelot, T. A.; Hu, C.-H.; Fowler, J. E.; DeLeeuw, B. J.; Schaefer, H. F., III. *J. Chem. Phys.* **1994**, *100*, 4347.
- (22) Vos, R. J.; Hendriks, R.; Van Duijneveldt, F. B. *J. Comput. Chem.* **1990**, *11*, 1.
- (23) Williams, I. H.; Spangler, D.; Femec, D. A.; Maggiora, G. M.; Schowen, R. L. *J. Am. Chem. Soc.* **1983**, *105*, 31.
- (24) Williams, I. H. *J. Am. Chem. Soc.* **1987**, *109*, 6299.
- (25) Nelander, B. *Chem. Phys.* **1992**, *159*, 281.
- (26) Nelander, B. *J. Chem. Phys.* **1980**, *72*, 77.
- (27) Zhang, X. K.; Lewars, E. G.; March, R. E.; Parnis, J. M. *J. Phys. Chem.* **1993**, *97*, 4320.
- (28) Stefanovich, E. V.; Truong, T. N. *J. Chem. Phys.* **1996**, *105*, 2961.
- (29) Kalapos, M. P. *Toxicol. Lett.* **1999**, *110*, 145.
- (30) Nemet, I.; Vikić-Topić, D.; Varga-Defterdarović, L. *Bioorg. Chem.* **2004**, *32*, 560.
- (31) Yaylayan, V. A.; Harty-Majors, S.; Ismail, A. A. *Carbohydr. Res.* **1998**, *309*, 31.
- (32) Malik, M.; Joens, J. A. *Spectrochim. Acta A* **2000**, *56*, 2653.
- (33) Frisch, M. J.; Trucks, G. W.; Schlegel, H. B.; Scuseria, G. E.; Robb, M. A.; Cheesman, J. R.; Montgomery, J. A., Jr.; Vreven, T.; Kudin, K. N.; Burant, J. C.; Millam, J. M.; Iyengar, S. S.; Tomasi, J.; Barone, V.; Mennucci, B.; Cossi, M.; Scalmani, G.; Rega, N.; Petersson, G. A.; Nakatsuji, H.; Hada, M.; Ehara, M.; Toyota, K.; Fukuda, R.; Hasegawa, J.; Ishida, M.; Nakajima, T.; Honda, Y.; Kitao, O.; Nakai, H.; Klene, M.; Li, X.; Knox, J. E.; Hratchian, J. P.; Cross, J. B.; Adamo, C.; Jaramillo, J.; Gomperts, R.; Stratmann, R. E.; Yazyev, O.; Austin, A. J.; Cammi, R.; Pomelli, C.; Ochterski, J. W.; Ayala, P. Y.; Morokuma, K.; Voth, G. A.; Salvador, P.; Dannenberg, J. J.; Zakrzewski, V. G.; Dapprich, S.; Daniels, A. D.; Strain, M. C.; Farkas, O.; Malick, D. K.; Rabuck, A. D.; Raghavachari, K.; Foresman, J. B.; Ortiz, J. V.; Cui, Q.; Baboul, A. G.; Clifford, S.; Cioslowski, J.; Stefanov, B. B.; Liu, G.; Liashenko, A.; Piskorz, P.; Komaromi, I.; Martin, R. L.; Fox, D. J.; Keith, T.; Al-Laham, M. A.; Peng, C. Y.; Nanayakkara, A.; Challacombe, M.; Gill, P. M. W.; Johnson, B.; Chen, W.; Wong, M. W.; Gonzales, C.; Pople, J. A. *GAUSSIAN 03, REVISION C.02*; Gaussian Inc.: Wallingford, CT, 2004.
- (34) Krishnan, R.; Binkley, J. S.; Seeger, R. S.; Pople, J. A. *J. Chem. Phys.* **1980**, *72*, 650.
- (35) Frisch, M. J.; Pople, J. A.; Binkley, J. S. *J. Chem. Phys.* **1984**, *80*, 3265.
- (36) Möller, C.; Plesset, M. S. *Phys. Rev.* **1934**, *46*, 618.
- (37) Binkley, J. S.; Pople, J. A. *Int. J. Quantum Chem.* **1975**, *9*, 229.
- (38) Boys, S. F.; Bernardi, F. *Mol. Phys.* **1970**, *19*, 553.
- (39) Shimanouchi, T. Tables of Molecular Vibrational Frequencies Consolidated Volume II. *J. Phys. Chem. Ref. Data* **1972**, *6*, 3, 993–1102.
- (40) Engdahl, A.; Nelander, B. *Chem. Phys. Lett.* **1988**, *148*, 264.
- (41) Diem, M.; MacDonald, B. G.; Lee, E. K. C. *J. Phys. Chem.* **1981**, *85*, 2227.
- (42) Gómez-Zavaglia, A.; Fausto, R. *J. Mol. Struct.* **2003**, *661*–662, 195.
- (43) Reid, S. A.; Kim, H. L.; McDonald, J. D. *J. Chem. Phys.* **1990**, *92*, 7079.
- (44) Dyllick-Brenzinger, C. E.; Bander, A. *Chem. Phys.* **1978**, *30*, 147.
- (45) Ayers, G. P.; Pullin, A. D. E. *Spectrochim. Acta A* **1976**, *32*, 1629; **1976**, *32*, 1689.
- (46) Fredin, L.; Nelander, B.; Ribbegard, G. *J. Chem. Phys.* **1977**, *66*, 4065; **1977**, *66*, 4073.
- (47) Bentwood, R. M.; Barnes, A. J.; Orville-Thomas, W. J. *J. Mol. Spectrosc.* **1980**, *84*, 391.
- (48) Barnes, A. J. *J. Mol. Struct.* **1990**, *237*, 19.
- (49) Hobza, P.; Havlas, Z. *Chem. Rev.* **2000**, *100*, 4253.
- (50) Barnes, A. J. *J. Mol. Struct.* **2004**, *704*, 3 and references therein.
- (51) Karpfen, A.; Kryachko, E. S. *Chem. Phys. Lett.* **2006**, *431*, 428 and references therein.